Forest Chemicals Review
www.forestchemicalsreview.com
ISSN: 1520-0191
March-April 2022 Page No. 161-174
Article History: Received: 08 February 2022, Revised: 10 March 2022, Accepted: 02 April 2022, Publication: 30 April 2022

Seasonal Variations of Tidal and Residual Currents Near the Pearl River Estuary

Tongmu Liu[1,2,3], Yonggang Cao[1,2*], Yan Wang[1], Jianxing Yu[3], Zaike Liu[4], Hua Huang[1,2], Xin-wen Zhang[1,2]

[1]South China Sea Marine Survey and Technology Center, State Oceanic Administration, Guangzhou, China
[2]Key Laboratory of Marine Environmental Survey Technology and Application, Ministry of Natural Resources, Guangzhou, China
[3]State Key Laboratory of Hydraulic Engineering Simulation and Safety, Tianjin University, Tianjin, China
[4]CNOOC Research Institute, Beijing, China
*Corresponding Author.

Abstract:

Quantifying the currents near the Pearl River Estuary is vital for understanding the circulation in the South China Sea. Based on the observational data of currents near the Pearl River Estuary from September 2017 to August 2018, the seasonal variations of tidal currents and residual currents at this point are analyzed. The results show that the tidal and current types in the west side of the Pearl River Estuary are irregular semidiurnal tides and irregular semidiurnal tidal currents. The diurnal O1 and K1 tide components show the characteristics of rotational flow. The half-day tidal component M2 and S2 are reciprocating. Ssa tidal component also contributes significantly. The residual current in the observed sea area is strong in autumn and winter, weak in spring and summer, strong in surface layer and weak in bottom layer, and the flow direction keeps southwest almost all year round. Especially during the southwest monsoon period in summer, the current along the west of the Pearl River Estuary presents the characteristics of adverse wind, and its velocity is about 10 cm/s.

Keywords*: South China Sea, Pearl River Estuary, Currents, Tidal currents, Residual currents.*

I. INTRODUCTION

The Pearl River Estuary in the South China Sea, near the China Greater Bay Area, is one of the busiest sea areas in terms of economic activities including marine engineering construction, fishery activities and shipping in China. Research for current features and variation is important to marine engineering construction, salvage, environmental protection and fishery production.

The geomorphic features of the Pearl River Estuary are complex with significant sea-land interaction. Affected by terrain, runoff and meteorological conditions of the Pearl River Estuary, the tides in this area are mainly formed by Pacific Ocean tidal waves entering the South China Sea into the estuary through the Luzon Strait [1]. Lin et al. (1996) analysed the Pearl River Estuary based on four large-scale synchronous observation and concluded that the estuary is a slightly counterclockwise reciprocating current, mainly

Forest Chemicals Review
www.forestchemicalsreview.com
ISSN: 1520-0191
March-April 2022 Page No. 161-174
Article History: Received: 08 February 2022, Revised: 10 March 2022, Accepted: 02 April 2022, Publication: 30 April 2022

dominated by irregular semidiurnal tidal currents [2]. Three tidal stations of the Pearl River Estuary are all irregular semidiurnal tides investigated by measured data [3]. Spatial distribution features of tidal current in the region near the estuary are available through numerical simulation research. FVCOM (finite volume coastal ocean model) simulation indicates that the tidal wave system in the South China Sea is dominated by the oceanic tidal waves introduced by the Bus Channel. The tidal types in the Pearl River Estuary are irregular semidiurnal tides and most of the continental shelf areas in the northern part of the South China Sea are irregular semidiurnal tidal currents [4]. The Pearl River Estuary is mainly alternating current with a northwest-southeast ellipse direction [5].

Southeast monsoon prevails in the northern part of the South China Sea in summer and it drives the northeast coastal currents. However, research shows that there is a westward coastal current in the west of the Pearl River Estuary throughout the year [6]. Xia et al. (2018) analysed the sectional observing data of the Pearl River Estuary in the summer of 2006 and found surface coastal high-current flowing westward in western Guangdong. Due to diffusion of diluted water, westward currents prevail and high-current exist in observed current velocity [7]. The coastal current in western Guangdong plays a decisive role in terrestrial substance (runoffs, nutrients and pollutants) migration and diffusion [6]. It is suggested that various factors including diluted water of the Pearl River, terrestrial runoff, upwelling and southeast wind field form the mechanism of westward coastal currents of west Guangdong in summer, but the dominant one is still unclear [8].

Most of the previous work is based on model output or short-term large sectional observation, while there are few researches studying long-term continuous current observation. Long-term continuous observed currents from September 2017 to August 2018 have been used to analyse the characteristics and time variations of tide, tidal current and residual current, aiming to increase the understanding of the hydrological status in this region and provide a certain reference for marine engineering construction and navigation safety.

II. MATERIALS AND METHODS

The analysing current materials in this paper were obtained from a 600kHz Acoustic Doppler Velocity Profiler (ADCP). The observation site is 113°26′ E, 21°30′ N, located 50 kilometers to southeast of the Pearl River Gaolan Island and its average water depth is about 27 meters (Fig 1). The ADCP observed upwards equipped on a seabed based observing system, with ten-minute ensemble interval, 0.5 meter observing cell unit and 1.6 meters blind zone from August 31, 2017 to June 26, 2018. The data during October 21, 2017 and November 14, 2017 lost caused by movement of observation system, affected by the twentieth typhoon 'Khanun' of 2017. Observation system was recovered and redeployed after the typhoon. The method was changed to submerged buoy observation equipped with 300kHz ADCP. It was set at 8 meters underwater with four-meter observing cell unit and six-meter blind zone. Valid data has been observed only from 14 meter to 18 meters water depth.

Forest Chemicals Review
www.forestchemicalsreview.com
ISSN: 1520-0191
March-April 2022 Page No. 161-174
Article History: Received: 08 February 2022, Revised: 10 March 2022, Accepted: 02 April 2022, Publication: 30 April 2022

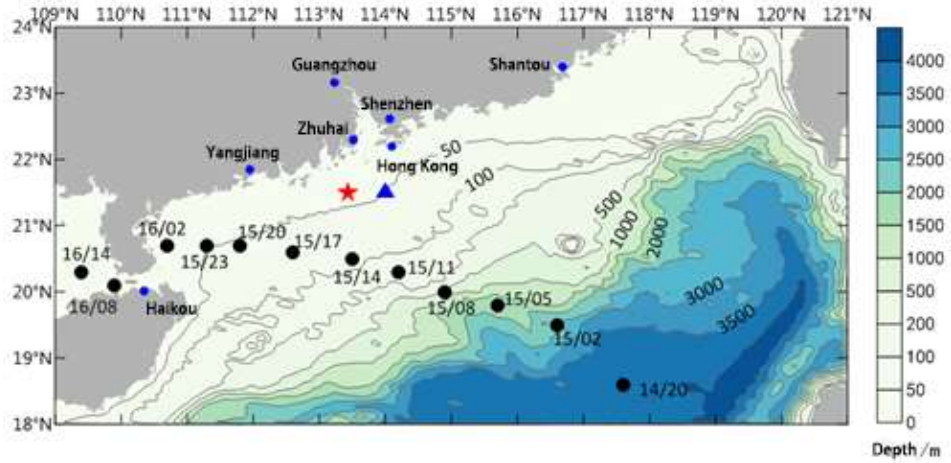

Fig 1: Geography of the northern South China Sea and location of the observation station

The red pentacle represents the observed site, blue triangle represents buoy site, black dots represent typhoon path of Khanun(××/×× represents date/time, e.g. 15/20 represents 2017/10/15 20:00).

Firstly, quality control of acquired data was performed referring to He et al. (2012) [9].

(1) the percentage of merit signal is less than 50%;

(2) the correlation value of the sound beam of transducer is less than 64;

(3) the vertical velocity is more than 40 cm/s;

(4) horizontal velocity is more than 300 cm/s;

(5) measurements that exceed 3 times the mean square relative error are considered as singular data and are excluded.

Lost data due to quality control were replaced by linear interpolation over time in order to facilitate the next process. The lost data from October 21, 2017 to November 14, 2017 have not been interpolated.

After quality control, the statistical characteristics of ocean currents were discussed using statistical analysis methods. T tide Program [10] was used to reconcile the tide and tidal data to get the tide and tidal features. Seasonal change characteristics of the residual currents were analysed finally.

Forest Chemicals Review
www.forestchemicalsreview.com
ISSN: 1520-0191
March-April 2022 Page No. 161-174
Article History: Received: 08 February 2022, Revised: 10 March 2022, Accepted: 02 April 2022, Publication: 30 April 2022

III. RESULTS

3.1 Statistical Analysis of Currents

The vector of profile current during observation period is showed in Fig 2. It has not been fully displayed as the long observing period. Low frequency vector of current shown in Fig 2 can be obtained conducting forty-eight-hour low pass filtering by an 2nd-order low-pass Butterworth filter. Vertical direction of the low frequency currents is basically the same due to relatively shallow water depth of the observation site. The value of velocity is gradually decreased from the surface to the bottom affected by the friction of the sea floor. The maximum low-frequency velocity is 108 cm/s occurred when the typhoon passed in terms of the autumn of 2017, while the maximum value appeared in January 2018 with a velocity of 60 cm/s in winter. The maximum value of Spring and Summer is found in April 2018 of 60 cm/s and June 2018 of 52 cm/s, respectively.

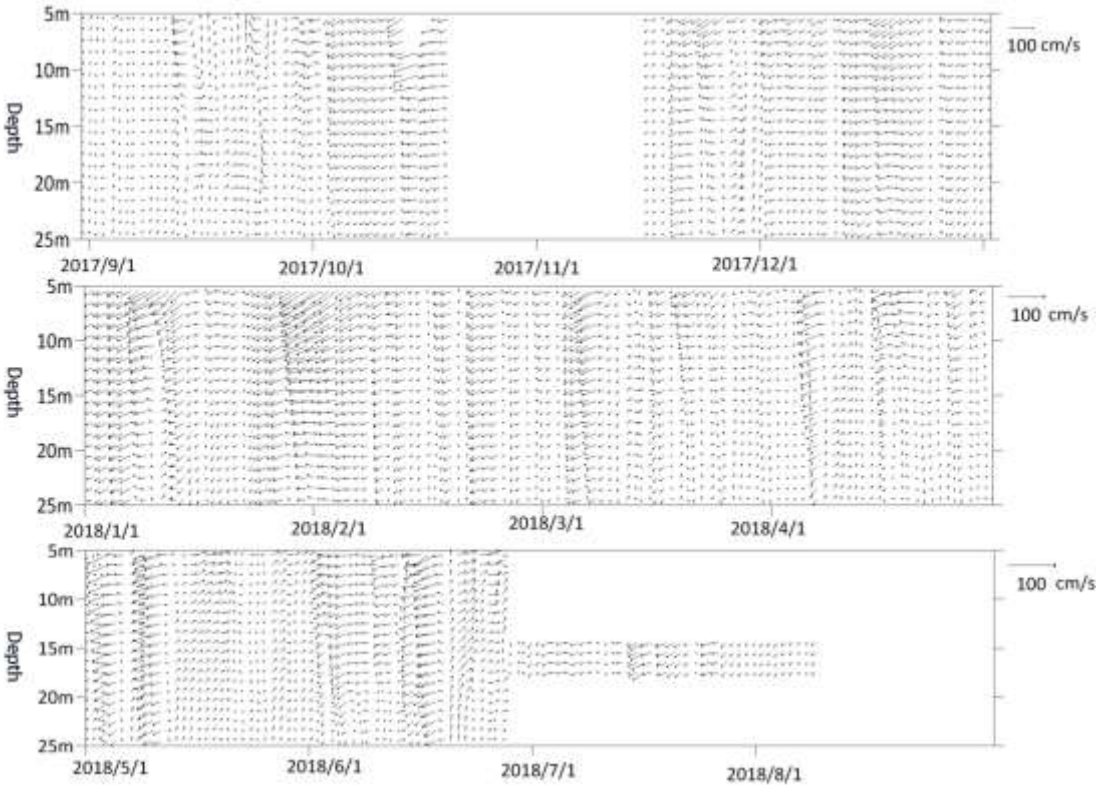

Fig 2: Daily average current. An 2nd-order low-pass Butterworth filter with 48h cutoff frequency has been performed

As shown in Fig 3, the distribution of current velocity and direction (unfiltered) has been estimated during observation period. It can be observed from the current-rose chart that the surface direction is dominated by WSW and SW, with frequency of 25% and 13%, respectively; the velocity is concentrated from 0 to 60 cm/s and from 60 to 90 cm/s, with frequency of 5%. The direction of WSW and W prevails in

Forest Chemicals Review
www.forestchemicalsreview.com
ISSN: 1520-0191
March-April 2022 Page No. 161-174
Article History: Received: 08 February 2022, Revised: 10 March 2022, Accepted: 02 April 2022, Publication: 30 April 2022

middle layer, contributing 24% and 17%, respectively; the velocity is mainly from 0 to 60 cm/s. The direction of bottom layer is dominated by WSW and SW, with frequency of 16% and 10%, respectively; the velocity is mainly from 0 to 30 cm/s.

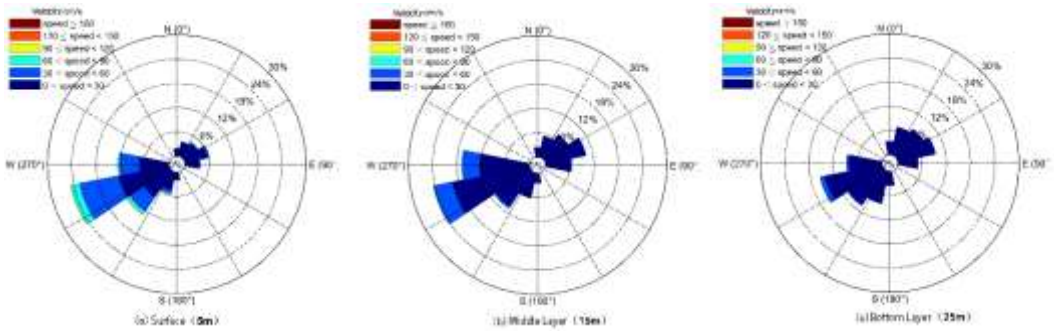

Fig 3: Current rose of the raw observational data

3.2 Tidal Analysis

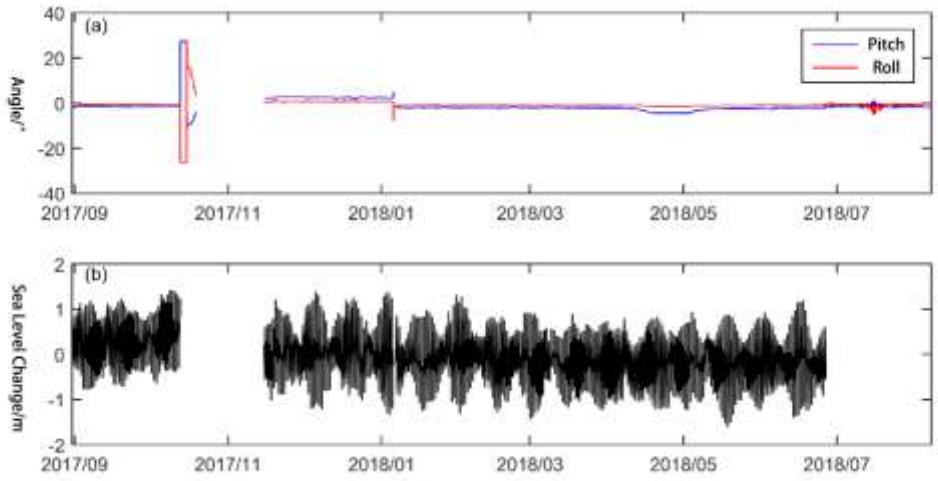

Fig 4: (a) Pitch and roll of ADCP; (b) time series of the sea level change

The quality of collecting data can be reflected by the pitch and roll sensor readings of the ADCP. The data is acceptable when the slope is within 15 degree, and the data quality is higher when the slope is within 5 degree. The ADCP pitch and roll were both within 5 degree during observation period excluding typhoon period (mid-October, 2017), which indicates the high quality of observational data (Fig 4 (a)).

Forest Chemicals Review
www.forestchemicalsreview.com
ISSN: 1520-0191
March-April 2022 Page No. 161-174
Article History: Received: 08 February 2022, Revised: 10 March 2022, Accepted: 02 April 2022, Publication: 30 April 2022

TABLE I. Harmonic constants of the main tidal constituents

Tidal constituents	Frequency/cph	Period/h	Amplitude/m	Angle/°
M2	0.0805	12.42	0.43	276.19
K1	0.0418	23.93	0.36	303.03
O1	0.0387	25.82	0.30	254.70
S2	0.0833	12.00	0.19	308.60
P1	0.0416	24.07	0.12	299.81
Ssa	0.0002	4382.91	0.10	209.42
N2	0.0790	12.66	0.09	256.85
Q1	0.0372	26.87	0.06	232.22

'cph' represents cycle per hour

The tidal changes can be reflected by the water depth measured by ADCP in seabed based observing system. As shown by change process of the water level in Fig 4 (b), the observed site presents a characteristic of semidiurnal tide - there are two high and low tides on a lunar day, while the height and time of adjacent high or low tides, showing the phenomenon of diurnal tide [3]. Harmonic analysis of observed site tidal data from November 15, 2017 to June 26, 2018 was conducted and harmonic constants of the main tidal constituents are shown in Table 1. The amplitude of the tidal constituents is M2, K1, O1, S2 in descending order. It is worth noting that the long observation time enable the amplitude of Ssa tidal constituents with 4382.9 hours (around 182.6 days) period to be given. The value of amplitude is around 0.1 meter, accounting for about a quarter of M2 constituent with a certain effect on the tidal level change. According to the ratio between the sum of two important diurnal constituents amplitude K1 and O1 and semidiurnal constituent amplitude M2 [10] - $F = \frac{H_{K_1}+H_{O_1}}{H_{M_2}}$ - the tides can be classfied into different types. The value of F can represent judging coefficient of tidal types if tidal amplitude is replaced by tidal current amplitude. It is calculated that F=1.5 in accordance with Table I, indicating that the tidal type of investigation site is irregular semidiurnal tide. This is close to measured [3] and simulated [4,5] result of adjacent region.

3.3. Current

3.3.1 Analysis of current rotation spectrum

The rotation spectrum of vector of different current layer are calculated to study the current variation features of the Pearl River Estuary varying with frequency (Fig 5). The current data observed from November 15, 2017 to June 26, 2018 were used to conduct rotation spectrum analysis because of data loss in other periods. It is shown from the Fig 5 that there are significant tidal constituent spectral peaks in the current vector rotation spectrum of each layer. With regard to semidiurnal constituent, the peak value

Forest Chemicals Review
www.forestchemicalsreview.com
ISSN: 1520-0191
March-April 2022 Page No. 161-174
Article History: Received: 08 February 2022, Revised: 10 March 2022, Accepted: 02 April 2022, Publication: 30 April 2022

corresponding to the M2 constituent is greater than that of diurnal constituent whereas the peak value of S2 constituent is less than that of diurnal constituent; the clockwise spectral peak of M2 constituent is greater than anti-clockwise one while they are close in terms of S2 constituent. As for diurnal constituent O1 and K1, the clockwise spectral peak of surface layer is greater than anti-clockwise one and they are basically the same in middle layer and the anti-clockwise spectral peak is higher in bottom layer. Therefore, the current energy of this area mainly concentrates on semidiurnal and diurnal cycle. With regard to the vertical diurnal constituent, the rotation is clockwise on the surface and middle layer while it is anti-clockwise on the bottom layer, while the clockwise rotational component of semidiurnal constituent is the same as the anti-clockwise one. In addition, the observation site with a relatively shallow depth is close to shore, so the spectral peak of the period (32.7h) corresponding to local inertial oscillations of the site is non-significant. Moreover, a significant spectral peak is noted for the M4 and Ms4 constituents, which represent harmonics of the M2 and S2 constituents due to shallow water effects. Significant spectral peak is noted from M4 and Ms4 period of shallow water current.

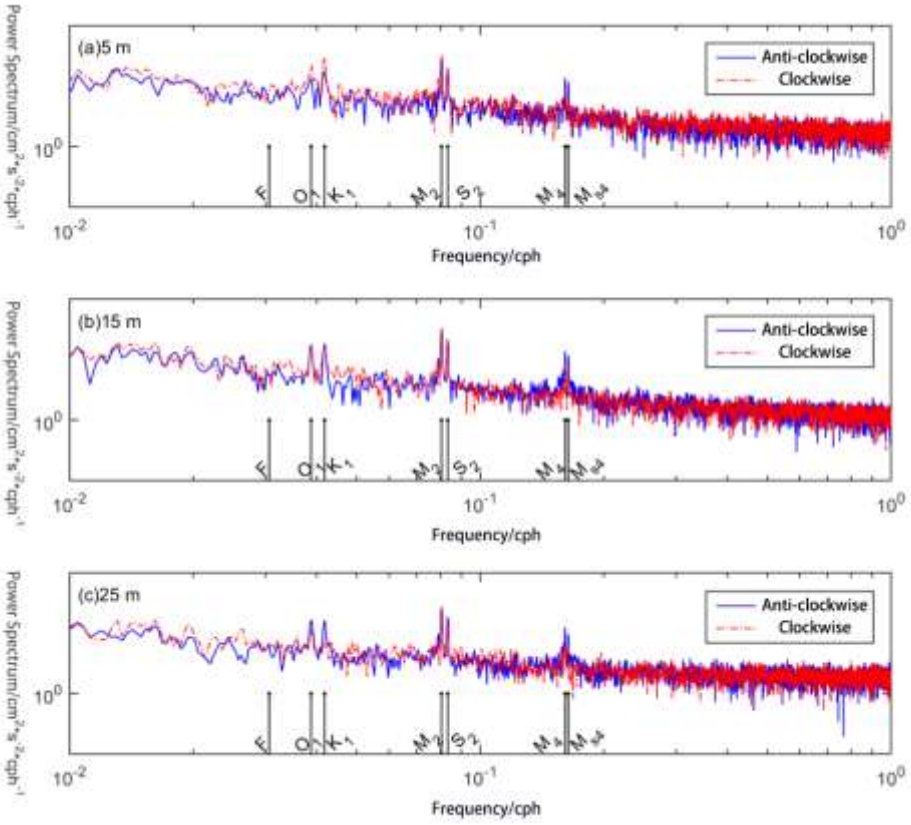

Fig 5: Rotation spectrum of the current (a) surface layer (b) middle layer (c) bottom layer
Blue/red line denotes anticlockwise/clockwise rotation.

Forest Chemicals Review
www.forestchemicalsreview.com
ISSN: 1520-0191
March-April 2022 Page No. 161-174
Article History: Received: 08 February 2022, Revised: 10 March 2022, Accepted: 02 April 2022, Publication: 30 April 2022

3.3.2 Harmonic analysis of current

The T tidal algorithm was used to perform harmonic analysis on the measured current data [11]. Tidal current ellipse and tidal current factor are shown in Fig 6 and Table II, respectively. The full-depth continuous observation data only between November 15, 2017 and June 29, 2018 has been analysed resulting from the lack of data lost from October to November, 2017.

Amplitudes of the main tidal constituents M2, S2, O1 and K1 decrease in sequence shown as Fig 6. The amplitude of M2 constituent is twice as large as the amplitudes of S2, O1, K1 constituents, and this result is the same as measured data of Mao [12] and simulation result of Ding [5] (2015). This area to type of tidal current is classified as irregular semidiurnal tidal current. The characteristic about constituents of diurnal cycle O1 and K1 is rotational current, rotating clockwise in surface layer and anti-clockwise in bottom layer. Meanwhile, semidiurnal constituent M2 and S2 are reciprocating with a non-significant rotation. The long axis direction of tidal current M2, S2, O1, K1 is Northeast-Southwest. The long cycle constituents are reciprocating with a direction of Northeast-Southwest, and the amplitude of constituents Ssa is close to the one of M2. Si (2012) proposed that the main constituent current near Dongsha Island in the Northern South China Sea comprises long cycle constituent Ssa and Msm on a basis of nine-month submerged buoy observation [13].

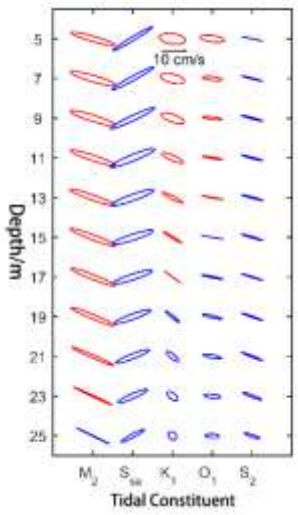

Fig 6: Tidal ellipse, blue/red line denotes anticlockwise/clockwise rotation

Forest Chemicals Review
www.forestchemicalsreview.com
ISSN: 1520-0191
March-April 2022 Page No. 161-174
Article History: Received: 08 February 2022, Revised: 10 March 2022, Accepted: 02 April 2022, Publication: 30 April 2022

TABLE II. Major axis, minor axis and inclination of the main tidal ellipse. Inclination is the angle between northern semi-major axis and East.

Depth /m	Constituent Current															Tpye
	Long Axis/(cm/s)					Short Axis/(cm/s)					Angle/°					
	M2	SSA	S2	O1	K1	M2	SSA	S2	O1	K1	M2	SSA	S2	O1	K1	
5	8.8	8.9	4.1	4.7	5.0	-1.0	0.7	0.0	-1.2	-2.0	164.0	31.0	167.6	172.7	171.9	1.11
7	9.0	9.2	4.2	4.0	4.8	-1.2	0.8	0.2	-0.7	-1.7	163.8	28.7	165.9	173.7	165.6	0.97
9	9.1	9.4	4.3	3.8	4.7	-1.2	1.0	0.3	-0.5	-1.5	162.6	25.3	165.2	173.5	160.6	0.93
11	9.2	9.3	4.3	4.0	4.5	-1.1	1.2	0.3	-0.3	-1.0	161.9	22.1	165.5	171.1	156.6	0.92
13	9.3	8.8	4.3	4.1	4.4	-1.0	1.2	0.3	-0.2	-0.6	160.7	19.7	165.1	170.2	152.4	0.91
15	9.3	8.3	4.3	4.2	4.2	-1.0	1.2	0.2	0.0	-0.3	159.5	17.9	163.8	170.3	148.1	0.90
17	9.2	7.9	4.3	4.1	3.9	-0.9	1.1	0.2	0.3	0.0	158.7	18.1	162.6	169.0	143.4	0.87
19	9.0	7.4	4.3	3.9	3.5	-0.8	1.0	0.2	0.5	0.4	157.6	19.6	160.4	167.1	141.2	0.81
21	8.8	6.9	4.2	3.6	3.0	-0.6	1.0	0.3	0.7	0.9	156.3	21.4	158.7	168.4	140.7	0.75
23	8.2	6.2	3.9	3.3	2.5	-0.3	0.9	0.4	0.8	1.2	154.8	23.8	158.9	174.2	141.1	0.70
25	6.9	5.1	3.1	2.6	1.8	0.1	0.7	0.5	0.8	1.3	153.8	28.2	161.2	177.4	137.2	0.65

Forest Chemicals Review
www.forestchemicalsreview.com
ISSN: 1520-0191
March-April 2022 Page No. 161-174
Article History: Received: 08 February 2022, Revised: 10 March 2022, Accepted: 02 April 2022, Publication: 30 April 2022

3.3.3 Residual current analysis

The residual currents of the Pearl River Estuary are mainly restricted by factors including runoff, coastal currents, wind currents and terrain [14]. The tidal currents have been excluded from original currents; then forty-eight-hour low pass filtering by an 2nd-order low-pass Butterworth filter have been conducted next aiming to obtain residual currents of observation site and investigate the seasonal change status about residual currents. Monthly average of residual currents is shown as Fig 7. It should be noticed that the observational data are only valid for 20 days, 17 days and 7 days in October and November, 2017 and August, 2018, respectively. The results of these months are not necessarily accurate, but it can roughly reflect the status about monthly residual currents.

As shown in Fig 7, autumn (from September to November, 2017) residual currents change significantly. In September, 2017, the surface of residual currents is westward while the middle and bottom layer are eastward; the velocity is relatively small and the maximum of middle layer is 5 cm/s. In October, the residual currents turn southwest and the velocity gradually decreases with the increase of water depth, the maximum of surface is 35 cm/s while the minimum of bottom layer is 12 cm/s. The velocity is greater in October mainly caused by onset of the Northeast monsoon and effect of typhoon. In November, the surface of the residual currents is Southwest with a maximum velocity of 26 cm/s and minimum velocity of 4 cm/s in the bottom. Affected by Northeast monsoon, the residual currents is strong with a surface velocity of 30 cm/s and bottom layer velocity of 10 cm/s in winter (from December, 2017 to February, 2018). The velocity is strongest in January flowing Southwestward from surface to bottom. For the increase of Northeast monsoon in Spring (from March to May, 2018), the residual currents reduce with maximum surface velocity of 15 cm/s but its direction is still Southwest. In Summer (from June to August, 2018), the velocity decrease to about 10 cm/s keeping a direction of West or Southwest. The average of residual currents among observation period is shown in Fig 8. The velocity gradually decrease from surface (16 cm/s) to bottom (3 cm/s) and the average direction is Southwest.

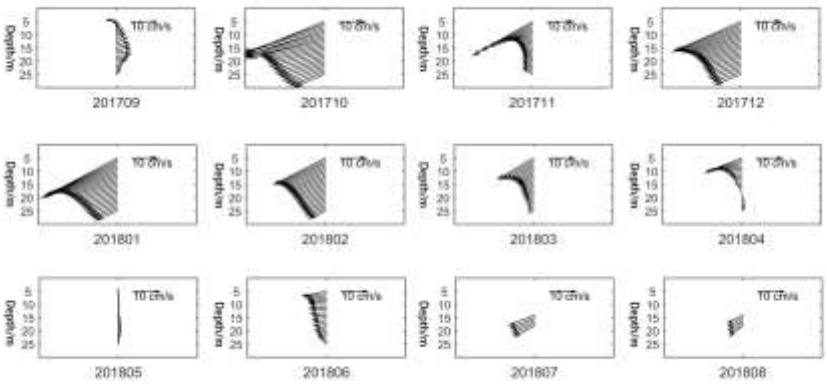

Fig 7: Monthly residual currents

Forest Chemicals Review
www.forestchemicalsreview.com
ISSN: 1520-0191
March-April 2022 Page No. 161-174
Article History: Received: 08 February 2022, Revised: 10 March 2022, Accepted: 02 April 2022, Publication: 30 April 2022

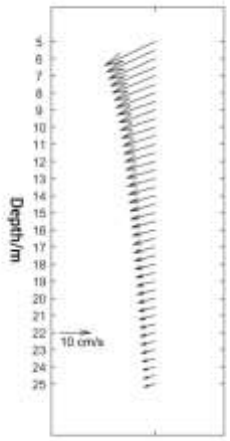

Fig 8: Average residual currents

An important part of the typhoon affecting surface ocean is the increase of mixed-layer velocity during the transit of the mixed-layer and the generation inertial flow after typhoon [15]. There were several typhoons pass through the target region during observation period. Case analysis has been conducted on residual currents during typhoon period with a huge influence. The twentieth typhoon "Kanu" of 2017 passed through northern part of the South China Sea from October 13 to 16, 2017. The typhoon center was only 100 kilometers away from the current and buoy observation site on October 15. In addition, the right side of its path significantly influenced the observational region. The wind and flow field was Northeast monsoon and Southwest stream before "Kanu" passed. The wind direction gradually turned to Northwest and the wind velocity was increased with approach of the low-pressure center of typhoon on October 13. The wind velocity of observation site reached 40 cm/s (shown as Fig 9(a)) on October 15 and the wind direction returned to Northeast. The direction of residual currents changed from 13 to 14 October. The velocity increased and the direction turned from Northwest to Southwest. The maximum velocity of 13th layer and 25th layer reached 1.82 and 0.8 cm/s, respectively. The near inertial oscillation caused by typhoon could last 5 to 10 days after the typhoon has passed in the region with shallow water. Period of the local-inertial frequency about observation site is 32.7 hours but the length of valid data after the typhoon was only four days which is from 16 to 20 October. The near-inertial energy comparison before and after the typhoon has not been performed resulting from the time span of valid observational data after typhoon, which was only four days from 16 to 20 October and not long enough for power spectrum analysis of current after typhoon.

Forest Chemicals Review
www.forestchemicalsreview.com
ISSN: 1520-0191
March-April 2022 Page No. 161-174
Article History: Received: 08 February 2022, Revised: 10 March 2022, Accepted: 02 April 2022, Publication: 30 April 2022

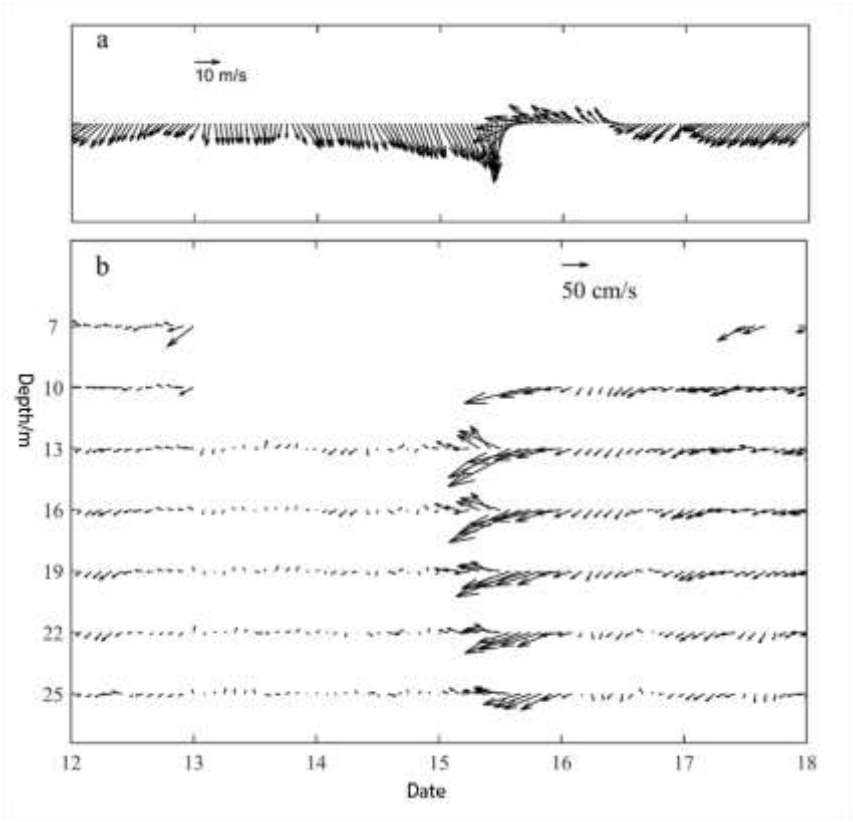

Fig 9: Wind velocity and residual currents during typhoon "KHANUN". The surface data was lost as large pitch and roll of seabed based observing system.

The residual currents in observation region is strong in autumn and winter compared to spring and summer and strong in surface compared to other layers. The direction of them is Southwest nearly all year round. Especially during Southwest monsoon in summer, the coastal currents to the west of the Pearl River Estuary are upwind with a velocity of 10 cm/s. This is almost the same as the observation result conducted by the predecessor [16]. Wu [17] and Yan and Chen [18] assumed that the Geostrophic Coriolis Force and southeast and east wind affecting the runoff of the Pearl River are the reason for the formation of coastal westward currents in west Guangdong. Seawater with low density piles up along the coast caused by summer runoff. Then this seawater flows to the west as the geostrophic effect. The most popular wind of west coast, meanwhile, is Southeast wind. The west coastal currents in west Guangdong are driven by both floatage and monsoon therefore. Yang et al. considered that there are two main factor - one is continental shelf rise causing temperature and salinity change of water and rainfall increase in summer [6]; another is land runoff input leading to sea level rise-affecting coastal current in west Guangdong and concluded it is Southwest monsoon in west coast by contrast. The main influence factors of west coastal currents in west Guangdong in summer, however, are still unsettled.

Forest Chemicals Review
www.forestchemicalsreview.com
ISSN: 1520-0191
March-April 2022 Page No. 161-174
Article History: Received: 08 February 2022, Revised: 10 March 2022, Accepted: 02 April 2022, Publication: 30 April 2022

IV. CONCLUSION

The feature of tide and tidal currents and the seasonal change of residual currents have been analysed on a basis of observational data from fixed-point station off the Pearl River from September, 2017 to August, 2018. The results indicated that it is irregular semidiurnal tide and irregular semidiurnal tidal current west off the Pearl River Estuary. Spectral analysis proved that the current energy mainly concentrates on semidiurnal and diurnal cycle; with regard to the vertical diurnal constituent, the rotation is clockwise on the surface and middle layer while it is anti-clockwise on the bottom layer, while the clockwise rotational component of semidiurnal constituent is the same as the anti-clockwise one. Meanwhile, the energy of local inertial oscillations is relatively weak. Significant spectral peak, in addition, is noted from long period and shallow period. The diurnal constituent O1 and K1 present a characteristic of rotational current while semidiurnal constituent M2 and S2 present a characteristic of reciprocating current. Ssa constituent also has great contribution. The residual currents in observation region is strong in autumn and winter compared to spring and summer and strong in surface compared to other layers. The direction of them is Southwest nearly all year round. Especially during Southwest monsoon in summer, the coastal currents to the west of the Pearl River Estuary are upwind with a velocity of 10 cm/s.

REFERENCES

[1] Zhang W, Ruan XH, Zheng JH, et al. (2010) Long-term change in tidal dynamics and its cause in the Pearl River Delta, China. Geomorphology 120(3-4): 209-223
[2] Lin ZH, Liang SH (1996) Tidal current analysis of the Pearl River Estuary. Marine Science Bulletin 15(2): 11-22
[3] Zhou, ZQ (2019) Analysis of wind and tidal characteristics in Pearl River Estuary based on measured data. Transactions of Oceanology and Limnology (1): 7
[4] Yang WK, Yi BS, Yang DZ, et al. (2013) Application of FVCOM in numerical simulation of tide and tidal currents in the northern South China Sea. Marine Sciences 37(9): 10-19
[5] Ding R, Chen XE, Qu ND (2015) Three-dimensional high-resolution numerical study of the tide and circulation in the Pearl River Estuary and its adjacent waters part I: model building and analysis. Periodical of Ocean University of China (11): 1-9
[6] Yang SQ, Bao XW, Chen CS, et al. (2003) Analysis on characteristics and mechanism of current system in west coast of Guangdong Province in the summer. Acta OCeanologica Sinica 25(6): 1-8
[7] Xia HY, Liu CJ, Wang DX (2018) The upwelling driven by the Zhujiang River runoff in 2006 summer. Haiyang Xuebao 40(7): 43-54
[8] Xie LL, Cao RX, Shang QT (2012) Progress of study on coastal circulation near the shore of western Guangdong. Journal of Guangdong Ocean University 32(4): 94-98
[9] He Q, Wei ZX, Wang YG (2012) Study on the sea currents in the northern shelf and slope of the South China Sea based on the observation. Acta Oceanologica Sinica 34(1): 17-28
[10] Fang GH (1986) Analysis and prediction of tide and tidal currents. Ocean Press. Beijing, China
[11] Pawlowicz R, Beardsley B, Lentz S (2002) Classical tidal harmonic analysis including error estimates in MATLAB using T_TIDE. Computers & Geosciences. 28(8): 929-937
[12] Mao QW, Shi P, Yin KD, et al. (2004) Tides and tidal currents in the Pearl River Estuary. Continental Shelf Research 24(16): 1797-1808

Forest Chemicals Review
www.forestchemicalsreview.com
ISSN: 1520-0191
March-April 2022 Page No. 161-174
Article History: Received: 08 February 2022, Revised: 10 March 2022, Accepted: 02 April 2022, Publication: 30 April 2022

[13] Si GC, Hou YJ (2012) The characteristics of the internal tides and residual tidal currents around the Dongsha Island in the northern South China Sea. Oceanologia Et Limnologia Sinica 43(1): 10-16
[14] Dong ZY, Li SQ, Sheng C (1985) Preliminary analysis of the residual current in the Zhujiang Estuary. Tropical Gegoraphy 5(3): 177-185.
[15] Zhu DY, Li L (2007) Near inertial oscillations in shelf-break of northern South China Sea after passage of typhoon Wayne. Journal of Tropical Oceanography (04): 3-9
[16] Yang Y, Li RX, Zhu PL, et al. (2014) Seasonal varaiation of the Pearl River diluted water and its dynamical cause. Marine Science Bulletin 33(1): 36-44
[17] Wu BJ (1990) A study on the circulation in the shelf waters west to Zhujiang River mouth II. Upwelling. Journal of Oceanography in Taiwan Strait (1): 2
[18] Yan JH, Chen DS (2005) The characteristics of low frequency currents in the area of Shuidong Anchored floating whelf in the west of Guangdong coastal waters. Transactions of Oceanology and Limnology (3): 8-15